

Observation of Low- and High-Energy Gamow-Teller Phonon Excitations in Nuclei

Y. Fujita,^{1,2,†} H. Fujita,¹ T. Adachi,¹ C. L. Bai,³ A. Algora,^{4,5} G. P. A. Berg,⁶ P. von Brentano,⁷ G. Colò,⁸ M. Csatlós,⁵ J. M. Deaven,⁹ E. Estevez-Aguado,⁴ C. Fransen,⁷ D. De Frenne,^{10,*} K. Fujita,¹ E. Ganioglu,¹¹ C. J. Guess,^{9,‡} J. Gulyás,⁵ K. Hatanaka,¹ K. Hirota,¹ M. Honma,¹² D. Ishikawa,¹ E. Jacobs,¹⁰ A. Krasznahorkay,⁵ H. Matsubara,^{1,§} K. Matsuyanagi,^{13,14} R. Meharchand,^{9,||} F. Molina,^{4,¶} K. Muto,¹⁵ K. Nakanishi,^{1,**} A. Negret,¹⁶ H. Okamura,^{1,*} H. J. Ong,¹ T. Otsuka,¹⁷ N. Pietralla,^{7,††} G. Perdikakis,^{9,18} L. Popescu,¹⁹ B. Rubio,⁴ H. Sagawa,^{12,13} P. Sarriguren,²⁰ C. Scholl,^{7,‡‡} Y. Shimbara,^{21,§§} Y. Shimizu,^{1,|||} G. Susoy,¹¹ T. Suzuki,¹ Y. Tameshige,¹ A. Tamii,¹ J. H. Thies,²² M. Uchida,¹ T. Wakasa,^{1,¶¶} M. Yosoi,¹ R. G. T. Zegers,⁹ K. O. Zell,⁷ and J. Zenihiro^{1,|||}

¹Research Center for Nuclear Physics, Osaka University, Ibaraki, Osaka 567-0047, Japan

²Department of Physics, Osaka University, Toyonaka, Osaka 560-0043, Japan

³Department of Physics, Sichuan University, Chengdu 610065, China

⁴Instituto de Física Corpuscular, CSIC-Universidad de Valencia, E-46071 Valencia, Spain

⁵Institute for Nuclear Research (MTA-Atomki), H-4001 Debrecen, Post Office Box 51, Hungary

⁶Department of Physics and JINA, University of Notre Dame, Indiana 46556, USA

⁷Institut für Kernphysik, Universität zu Köln, D-50937 Köln, Germany

⁸Dipartimento di Fisica, Università degli Studi di Milano, and INFN, Sezione di Milano, via Celoria 16, 20133 Milano, Italy

⁹National Superconducting Cyclotron Laboratory, Michigan State University, East Lansing, Michigan 48824-1321, USA

¹⁰Vakgroep Subatomaire en Stralingsfysica, Universiteit Gent, B-9000 Gent, Belgium

¹¹Department of Physics, Istanbul University, Istanbul 34134, Turkey

¹²Center for Mathematical Sciences, University of Aizu, Aizu-Wakamatsu, Fukushima 965-8580, Japan

¹³RIKEN, Nishina Center, Wako Saitama 351-0198, Japan

¹⁴Yukawa Institute for Theoretical Physics, Kyoto University, Kyoto 606-8502, Japan

¹⁵Department of Physics, Tokyo Institute of Technology, Ohokayama, Meguro, Tokyo 152-8551, Japan

¹⁶Horia Hulubei National Institute for Physics and Nuclear Engineering, 077125 Bucharest-Magurele, Romania

¹⁷Department of Physics, University of Tokyo, Hongo, Bunkyo, Tokyo 113-0033, Japan

¹⁸Department of Physics, Central Michigan University, Mt. Pleasant, Michigan 48859, USA

¹⁹SCK-CEN, Belgian Nuclear Research Center, B-2400 Mol, Belgium

²⁰Instituto de Estructura de la Materia, IEM-CSIC, Serrano 123, E-28006 Madrid, Spain

²¹Graduate School of Science and Technology, Niigata University, Nishi, Niigata 950-2181, Japan

²²Institut für Kernphysik, Westfälische Wilhelms-Universität, D-48149 Münster, Germany

(Received 29 January 2014; published 18 March 2014)

Gamow-Teller (GT) transitions in atomic nuclei are sensitive to both nuclear shell structure and effective residual interactions. The nuclear GT excitations were studied for the mass number $A = 42, 46, 50$, and 54 “ f -shell” nuclei in (^3He , t) charge-exchange reactions. In the $^{42}\text{Ca} \rightarrow ^{42}\text{Sc}$ reaction, most of the GT strength is concentrated in the lowest excited state at 0.6 MeV, suggesting the existence of a low-energy GT phonon excitation. As A increases, a high-energy GT phonon excitation develops in the 6–11 MeV region. In the $^{54}\text{Fe} \rightarrow ^{54}\text{Co}$ reaction, the high-energy GT phonon excitation mainly carries the GT strength. The existence of these two GT phonon excitations are attributed to the 2 fermionic degrees of freedom in nuclei.

DOI: [10.1103/PhysRevLett.112.112502](https://doi.org/10.1103/PhysRevLett.112.112502)

PACS numbers: 24.30.Cz, 25.55.Kr, 27.40.+z

Atomic nuclei are the “quantum finite many-body system” consisting of correlated nucleons, i.e., protons and neutrons. However, the independent particle model called the shell model (SM), has succeeded in describing single “particle (p)” or single “hole (h)” properties of a proton (π) or a neutron (ν). By introducing a spin-orbit ($L \cdot S$) force, whose effect is stronger than in atoms, the shell closures at “magic numbers” (the proton number Z or neutron number N of 2, 8, 20, 28, and so forth [see, e.g., Ref. [1]]) were reproduced. The “doubly magic nuclei” such as ^4He with $N = Z = 2$, ^{16}O with $N = Z = 8$, or ^{40}Ca with $N = Z = 20$ behave like an atomic inert gas, and can work as inert cores.

Nucleons can also form strongly correlated pairs [2,3]. These nuclear correlations can be treated as effective residual interactions (ERIs). The collective excitations caused by ERIs are commonly observed in many-body systems. In nuclei, giant resonances (GRs) with specific total angular momentum and parity (J^π values) are examples. They are visualized as one-phonon vibrations from a macroscopic view point, or as collective excitations of particle-hole (p - h) or particle-particle (p - p) configurations from a microscopic view point [4]. Note that nucleons have a spin degree of freedom. In addition, they have two “faces,” i.e., π and ν . In 1932, Heisenberg introduced the isospin quantum number T to describe phenomena caused

by the 2 fermionic degrees of freedom. Therefore, GRs as well as ERIs can be specified by their spin nonflip and spin flip nature and, also, by the isoscalar (IS) and the isovector (IV) characters. In IV excitations, πs and νs vibrate out of phase. Note that they are found only in systems having 2 fermionic degrees of freedom. In this respect, Gamow-Teller (GT) excitations specified by both spin and IV excitations are characteristic of nuclei.

Only a few configurations are involved in GT transitions caused by the GT operator $\sigma\tau$ having no radial or angular momentum component [5,6]. In a SM picture, where the nucleons are in an orbit with angular momentum ℓ and spin $s = \pm 1/2$, GT transitions can connect only the orbits with the $j_> (= \ell + 1/2)$ and $j_< (= \ell - 1/2)$ values, where the former is energetically lower than the latter due to the $L \cdot S$ force. Therefore, without ERIs, a transition between $j_>$ orbits causes an excitation at zero energy, while a $j_> \rightarrow j_<$ transition occurs at 3 to 7 MeV [1].

Absolute values of GT transition strength $B(\text{GT})$ can be obtained in β -decay studies. The accessible excitation energy (E_x), however, is limited by the decay Q value [6]. In the 1980s, it was found that charge-exchange (CE) reactions at intermediate incident energies ($E > 100$ MeV/nucleon) and the scattering angle $\Theta = 0^\circ$ are good tools for the study of GT excitations [4]. In the studies using (p, n) reactions [7], bumplike GT resonances (GTRs), i.e., high-energy GT phonon excitations, with a few MeV width were commonly observed at $E_x = 9$ –18 MeV in nuclei with mass A larger than about 60 [7,8]. The main part of the GT strength was carried by the GTRs containing ≈ 50 –60% of the GT sum-rule strength [8]. Note that GTRs were always observed at E_x s higher than the energy difference of the $j_<$ and $j_>$ orbits. Because of the neutron excess in these nuclei, the main configurations of the GTRs are of p - h nature. It is well established that the ERIs among the p - h configurations in IV excitations, such as the GT or IV dipole excitations, have a repulsive nature, and thus, IV GRs are pushed up relative to the unperturbed p - h energies [4]. On the contrary, in lighter nuclei with mass number $A \leq 40$, prominent high-energy GTRs are not observed; the GT strength is mainly carried by states at lower energies [6,7]. This raises a question of how these two features of GT strength distributions can be understood consistently.

In order to reconcile these observations, we studied the GT excitations for the “ f -shell” nuclei in the transitional mass region of $40 < A < 60$ using the (p, n) -type (${}^3\text{He}, t$), CE reaction. The orbits $f_{5/2}$ and $f_{7/2}$ with $\ell = 3$ represent the $j_<$ and $j_>$ orbits, respectively, where the single particle energy of the former is about 6 MeV higher than that of the latter [1]. For a systematic study, we selected target nuclei with even Z and N numbers and neutron excesses of two, i.e., $T_z = +1$, where $T_z = (N - Z)/2$ is the z component of isospin T . They were ${}^{42}\text{Ca}$, ${}^{46}\text{Ti}$, ${}^{50}\text{Cr}$, and ${}^{54}\text{Fe}$. The final nuclei are ${}^{42}\text{Sc}$, ${}^{46}\text{V}$, ${}^{50}\text{Mn}$, and ${}^{54}\text{Co}$ with odd Z and N numbers and $T_z = 0$, respectively.

It has been shown that GT excitations dominate the spectra of the (${}^3\text{He}, t$), CE reaction at 0° and an intermediate beam energy of 140 MeV/nucleon [6]. In addition, although there were exceptions, a close proportionality between the cross sections at 0° and the $B(\text{GT})$ values

$$\sigma(0^\circ) \approx \delta^{\text{GT}}(0^\circ)B(\text{GT}), \quad (1)$$

has been empirically established [6,9–13], where $\delta^{\text{GT}}(0^\circ)$ is the unit GT cross section at 0° .

The (${}^3\text{He}, t$) experiments were performed at the high resolution facility of RCNP, consisting of a beam line WS course [14] and the Grand Raiden spectrometer [15] using the ${}^3\text{He}$ beam from the $K = 400$ Ring Cyclotron [16]. The targets consisted of enriched self-supporting ${}^{42}\text{Ca}$, ${}^{46}\text{Ti}$, ${}^{50}\text{Cr}$, and ${}^{54}\text{Fe}$ metal foils with thicknesses of 0.8–1.8 mg/cm². The outgoing tritons were momentum analyzed within the full acceptance of the spectrometer at 0° and detected with a focal-plane detector system [17].

Energy resolutions of $\Delta E = 21$ –33 keV (FWHM), much better than the energy spread of the beam of about 120 keV, were realized by applying both dispersion matching and focus matching techniques [6,18,19]. These resolutions are about 1 order of magnitude better than those in the pioneering (p, n) works [7,20,21]. This high energy resolution makes a detailed study of GT excitations possible. A good angular resolution of $\Delta\Theta \leq 5$ mr (FWHM) was achieved by applying the angular dispersion matching technique [18] and the overfocus mode of the spectrometer [22].

The acceptance of the spectrometer was subdivided into four scattering-angle regions of $\Theta = 0^\circ$ – 0.5° , 0.5° – 1.0° , 1.0° – 1.5° , and 1.5° – 2.0° using the tracking information. The $J^\pi = 1^+$, GT states excited by $\Delta L = 0$, GT transitions can be identified by their maximum intensity at $\Theta = 0^\circ$ (for detail, see [23]). Figure 1 shows the “ 0° spectra” that include the events with $\Theta \leq 0.5^\circ$. The ${}^{46}\text{V}$, ${}^{50}\text{Mn}$, and ${}^{54}\text{Co}$ spectra are from Refs. [23–25], and the ${}^{42}\text{Ca}({}^3\text{He}, t){}^{42}\text{Sc}$ spectrum was newly measured in this study. The angular distribution analysis shows that most of the prominent states are excited with $\Delta L = 0$. Among them, the ground states are all $J^\pi = 0^+$ isobaric analog states (IASs), each forming an isospin multiplet with the target ground state. Therefore, it is suggested that the $\Delta L = 0$ excited states are $J^\pi = 1^+$, GT states [6]. The $B(\text{GT})$ values were derived using Eq. (1). The δ^{GT} values were deduced by using the information on the $T_z = -1 \rightarrow 0, \beta^+$ decay [25,26] assuming that $T_z = \pm 1 \rightarrow 0$ mirror GT transitions have the same $B(\text{GT})$ values on the basis of isospin symmetry [6]. The gradual decrease of δ^{GT} as a function of E_x [9] was corrected using distorted wave Born approximation calculations (see, e.g., [23]).

The remarkable feature in Fig. 1 is the completely different strength distributions in these four systems although the neutron excess in the initial nuclei is always

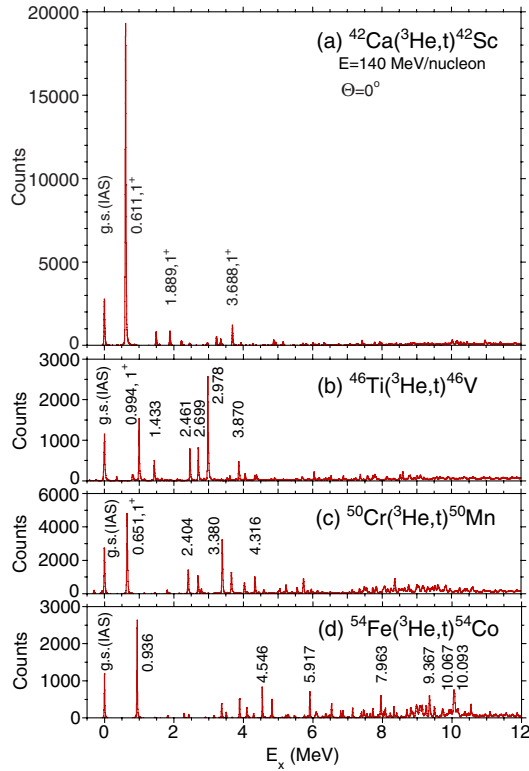


FIG. 1 (color online). High energy-resolution spectra of $(^3\text{He}, t)$ reaction on $A = 42\text{--}54$, $T_z = +1$ target nuclei. The vertical scales are normalized so that the heights of all GT peaks are approximately proportional to the $B(\text{GT})$ values. The GT strength is concentrated in one low-energy state in ^{42}Sc [panel (a)]. The fine structures of GTRs in the 6–11 MeV region are observed in panels (c) and (d).

two. In ^{42}Sc , most of the GT strength, in agreement with [20], is concentrated in the excitation of the lowest GT state at 0.611 MeV. In ^{46}V and ^{50}Mn , however, the low-energy strength becomes fragmented and at the same time the bumplike structure of the GTR in the 6–11 MeV region begins to develop [Figs. 1(b) and 1(c)]. A fragmentation of GT strength was also observed in the $^{44}\text{Ca} \rightarrow ^{44}\text{Sc}$ reaction [27], suggesting that the concentration of the strength is also hampered by a larger neutron excess of four in ^{44}Ca . Finally in ^{54}Co [Fig. 1(d)], the GT strength is mainly in the GTR.

The cumulative sum of the experimental $B(\text{GT})$ values is shown in Fig. 2(a) up to $E_x = 12$ MeV. A shift in the strength to higher energy with increasing A is again clearly seen. The total sum in ^{42}Sc is 2.7(4), with 80% of the GT strength carried by the lowest GT state. The observed sum gradually increases with A and it is 3.9(6) in ^{54}Co [23], where $\approx 75\%$ of the GT strength is found in the high-energy GTR structure.

In a SM picture, the $j_>$ valence orbits, $\pi f_{7/2}$ and $\nu f_{7/2}$, outside the inert ^{40}Ca core ($Z = N = 20$) will be gradually filled in the $T_z = +1$, $A = 42\text{--}54$ nuclei as A increases (see Fig. 3). On the other hand, the $j_<$, $\pi f_{5/2}$ and $\nu f_{5/2}$ orbits

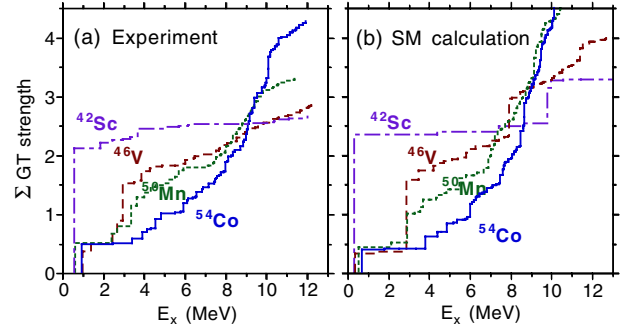


FIG. 2 (color online). (a) Cumulative-sum strengths of the experimental $B(\text{GT})$ values in the final nuclei ^{42}Sc , ^{46}V , ^{50}Mn , and ^{54}Co . They are shown by dotted-dashed, dashed, dotted, and solid lines, respectively. (b) Cumulative sums from SM calculations [28] including the quenching factor of $(0.74)^2$.

remain unpopulated. In this picture, without ERIs, we expect a low-energy GT excitation originating from the $\nu f_{7/2} \rightarrow \pi f_{7/2}$ transition and a high-energy one from the $\nu f_{7/2} \rightarrow \pi f_{5/2}$, where the latter is expected ≈ 6 MeV higher than the former due to the strong $L \cdot S$ force [1]. The single particle strengths of these GT excitations are similar, namely $B(\text{GT}) = 9/7$ and $12/7$, respectively [9]. Taking into account the occupation and vacancy factors of the $f_{7/2}$ and $f_{5/2}$ shells, the relative strengths between the $\nu f_{7/2} \rightarrow \pi f_{7/2}$ and $\nu f_{7/2} \rightarrow \pi f_{5/2}$ transitions are 9:12 and 9:48 in the $^{42}\text{Ca} \rightarrow ^{42}\text{Sc}$ and $^{54}\text{Fe} \rightarrow ^{54}\text{Co}$ reactions, respectively. Therefore, we can, to some extent, understand the larger high-energy strength in the $A = 54$ system. However, from this simple picture, we cannot understand the concentration of GT strength to the low-energy 0.611 MeV state in the $^{42}\text{Ca} \rightarrow ^{42}\text{Sc}$ reaction.

Figure 2(b) shows the cumulative sum of the GT strengths from SM calculations. The modern GXPF1J interaction used in the calculation was derived to reproduce various experimental data [28]. We see that the A dependence of the GT strength distribution, including the

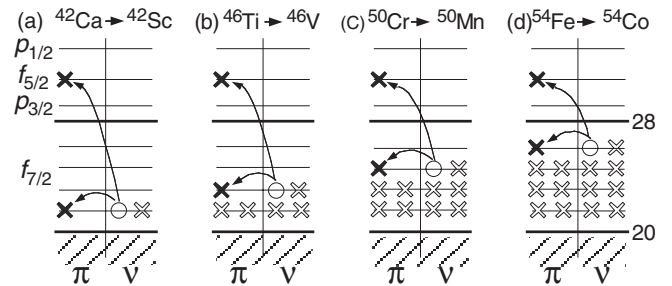


FIG. 3. The SM configurations before and after the β^- -type GT transitions in $A = 42\text{--}54$, f -shell nuclei. Positions occupied by protons (π) and neutrons (ν) are shown by open crosses. Positions that are newly occupied by protons and unoccupied by neutrons after making GT transitions (shown by the arrows) are indicated by filled crosses and open circles, respectively. The shell closures at $Z = N = 20$ and 28 are indicated by thick solid lines.

concentration of the GT strength in the lowest GT state in ^{42}Sc , is well reproduced. However, we notice that this concentration of the GT strength is reproduced even in a SM calculation using the classical Kuo-Brown interaction [29], suggesting that it contains the essential ERI components that make the GT strength concentrate in the lowest GT state of ^{42}Sc .

Further calculations were performed using a quasiparticle random phase approximation (QRPA) framework based on a self-consistent Hartree-Fock mean field with Skyrme interactions. First, we performed standard calculations including proper IV ERIs in both the p - h and the p - p configurations. Within this framework, GT strengths and GTR structures in nuclei heavier than $A \approx 60$ have been well reproduced [30]. As an extension, the observed GT strength in the GTR region of ^{54}Co was well reproduced. Note that closed shells are formed at Z or $N = 28$. Then, the main transition $\nu f_{7/2} \rightarrow \pi f_{5/2}$ makes a p - h type ($\pi f_{5/2}$, $\nu f_{7/2}^{-1}$) configuration in ^{54}Co [see Fig. 3(d)]. Here, we see the established scenario that the main part of the GT strength is pushed up to the GTR region, higher than the p - h energy of ≈ 6 MeV, by the repulsive IV interaction that is active in p - h configurations. However, the concentration of GT strength in one low-energy state in ^{42}Sc could not be reproduced; about half of the total GT strength always remained in the GTR region.

In the SM picture, the final nucleus ^{42}Sc has one π and one ν outside the inert ^{40}Ca core. As shown in Fig. 3(a), p - p configurations of ($\pi f_{7/2}$, $\nu f_{7/2}$) and ($\pi f_{5/2}$, $\nu f_{7/2}$), are formed after the transitions $\nu f_{7/2} \rightarrow \pi f_{7/2}$ and $\nu f_{7/2} \rightarrow \pi f_{5/2}$, respectively. Taking the antisymmetrization into account, a π - ν pair can couple to the spin $S = 0$ and $T = 1$ (spin-singlet, IV) or $S = 1$ and $T = 0$ (spin-triplet, IS) states, and the analysis of ERIs in these states shows that the spin-triplet IS ERI is attractive and stronger than the spin-singlet IV ERI [31]. Note that the IS, ERI cannot act in the IV-type π - π or ν - ν pairs. In addition, it is discussed that p - p type configurations are sensitive to the IS pairing interaction [32,33], and the attraction is strong if both nucleons of the π - ν pair are in the same shell [3,31]. It is known that this attractive IS ERI makes the deuteron bound [34].

In newly performed spherical QRPA calculations [35], the spin-triplet IS ERI was also included, which changed the results drastically; in the $^{42}\text{Ca} \rightarrow ^{42}\text{Sc}$ calculation, a strong concentration of the GT strength in the lowest GT state appeared as the IS coupling constant f [35] was increased from null to $f = 1$. In addition, at $f = 1$ the contributions of the main p - p type configurations ($\pi f_{5/2}$, $\nu f_{7/2}$) and ($\pi f_{7/2}$, $\nu f_{7/2}$) of the lowest 1^+ state were in phase, increasing the collectivity [35].

As discussed, the configurations of GTRs are p - h type in heavier nuclei with neutron excess. Since ERIs of p - h configurations are repulsive in IV excitations, the GTRs are pushed to a higher E_x region. However, we observed that

the GT excitations can be shifted to a lower energy if the configurations of the final nucleus have πp - νp nature where the attractive IS ERI can be active. We saw that the 0.611 MeV GT state in ^{42}Sc collects 80% of the total GT strength in the region up to 12 MeV. The GT transition to this state has a large $B(\text{GT})$ value of 2.2, which can be deduced from the small $\log ft$ value of 3.25 of the isospin analogous GT transition in the ^{42}Ti β decay to ^{42}Sc [36]. Therefore, in the sense that this low-energy GT state has the collective nature and carries most of the observed GT strength, it is comparable to the high-energy GTR in heavy $N > Z$ nuclei.

In the limit of null $L \cdot S$ force, Wigner proposed the existence of SU(4) symmetry and the “super-multiplet state” [37]. In this limit, (a) the GT strength is concentrated in a low-energy GT state, and, also, (b) excitation energies of both the IAS and the GT state are identical. From Fig. 1, we see a broken SU(4) symmetry in the $A = 54$ system, while a good symmetry is observed in the $A = 42$ system. We found that the attractive IS ERI plays the role of restoring the SU(4) symmetry and the 0.611 MeV GT state in ^{42}Sc has a character close to that of a super-multiplet state. Therefore, we can call this state the “low-energy super GT” (LESGT) state. Note that “zero-energy” πp - νp configurations that are essential for the formation of LESGT states are realized only in CE excitations (and β decays).

The LESGT state is expected if the relevant configurations of the final GT state are of πp - νp nature. Indeed, strong GT transitions to the ground states of the $N = Z$ nuclei ^6Li and ^{18}F have been observed in the β -decay studies of ^6He and ^{18}Ne , respectively [38,39]. The transitions have very small $\log ft$ values of 2.9 and 3.1. In addition, we can confirm the concentration of the main GT strength in the ground state of ^{18}F from the $^{18}\text{O}(p, n)$ measurement [40]. Since ^4He and ^{16}O can act as inert cores, we expect that these ground states in ^6Li and ^{18}F have πp - νp configurations, and thus, they are also LESGT states.

In summary, in the high-resolution (^3He , t) measurements for f -shell nuclei, we observed low- and high-energy collective GT excitations, i.e., two kinds of GT phonon states. In ^{42}Sc , a concentration of the GT strength was observed in the lowest GT state, which we call the LESGT state. We found that the attractive IS ERI that is active in πp - νp configurations pulls the GT strength to a lower excitation energy and that LESGT states are the extreme structure carrying most of the GT strength. In ^{46}V and ^{50}Mn , transitional features were observed; the low-energy phonon strength became fragmented and weaker, while the strength in the high-energy GTR region increased. In ^{54}Co , the main part of the GT strength was concentrated in the GTR phonon structure. As is known, GTRs are formed by the repulsive IV ERI that is active in the πp - νh configurations. Note that the existence of IS and IV ERIs, and thus, low- and high-energy GT phonon excitations, are attributed

to the 2 fermionic degrees of freedom, which is a unique feature in atomic nuclei.

The (^3He , t) experiments were performed at RCNP, Osaka under the Experimental Programs No. E197, No. E214, and No. E307. Y. F. acknowledges discussions with Professors H. Toki (Osaka), I. Hamamoto (University of Lund), M. H. Harakeh (KVI), and W. Gelletly (Surrey). This work was in part supported by MEXT, Japan (Grants No. 13002001, No. 15540274, and No. 18540270); MICINN, Spain (Grant No. FPA200806419-C02-01); DFG, Germany (Contracts No. Br 799/12-1, No. Jo 391/2-1, and No. Pi 393/1-2); the FWO-Flanders, OTKA Foundation, Hungary (Grant No. K106035); and RIKEN-CNS joint research project on large-scale nuclear-structure calculations. Y. F. and B. R. acknowledge the support of the Japan-Spain collaboration program by JSPS and CSIC.

*Deceased.

†fujita@rcnp.osaka-u.ac.jp

‡Present address: Department of Physics and Applied Physics, University of Massachusetts Lowell, Lowell, Massachusetts 01854, USA.

§Present address: NIRS, Inage, Chiba 263-8555, Japan.

||Present address: Los Alamos National Laboratory, Los Alamos, New Mexico 87545, USA.

¶Present address: Comisión Chilena de Energía Nuclear, Post Office Box 188-D, Santiago, Chile.

**Present address: Central Customs Laboratory, Ministry of Finance, Kashiwa, Chiba 277-0882, Japan.

††Present address: IKP, TU-Darmstadt, Darmstadt, Germany.

‡‡Present address: Institute for Work Design of North Rhine-Westphalia, Radiation Protection Services, 40225 Düsseldorf, Germany.

§§Present address: CYRIC, Tohoku University, Aramaki, Aoba, Sendai 980-8578, Japan.

|||Present address: RIKEN, Nishina Center, Wako, Saitama 351-0198, Japan.

¶¶Present address: Department of Physics, Kyushu University, Higashi, Fukuoka 812-8581, Japan.

- [1] A. Bohr and B. R. Mottelson, *Nuclear Structure* (Benjamin, New York, 1969), Vol. 1.
- [2] R. A. Broglia and V. Zelevinsky, *Fifty Years of Nuclear BCS, Pairing in Finite Systems* (World Scientific, Singapore, 2013).
- [3] R. Subedi *et al.*, *Science* **320**, 1476 (2008), and references therein.
- [4] M. N. Harakeh and A. van der Woude, *Giant Resonances, Oxford Studies in Nuclear Physics* (Oxford University Press, Oxford, 2001), and references therein.
- [5] F. Osterfeld, *Rev. Mod. Phys.* **64**, 491 (1992), and references therein.
- [6] Y. Fujita, B. Rubio, and W. Gelletly, *Prog. Part. Nucl. Phys.* **66**, 549 (2011), and references therein.
- [7] J. Rapaport and E. Sugarbaker, *Annu. Rev. Nucl. Part. Sci.* **44**, 109 (1994), and references therein.

- [8] C. Gaarde, *Nucl. Phys.* **A396**, 127c (1983).
- [9] T. N. Taddeucci, C. A. Goulding, T. A. Carey, R. C. Byrd, C. D. Goodman, C. Gaarde, J. Larsen, D. Horen, J. Rapaport, and E. Sugarbaker, *Nucl. Phys.* **A469**, 125 (1987), and references therein.
- [10] Y. Fujita *et al.*, *Phys. Rev. C* **59**, 90 (1999).
- [11] Y. Fujita *et al.*, *Phys. Rev. C* **67**, 064312 (2003).
- [12] R. Zegers *et al.*, *Phys. Rev. C* **74**, 024309 (2006).
- [13] Y. Fujita *et al.*, *Phys. Rev. C* **75**, 057305 (2007).
- [14] T. Wakasa *et al.*, *Nucl. Instrum. Methods Phys. Res., Sect. A* **482**, 79 (2002).
- [15] M. Fujiwara *et al.*, *Nucl. Instrum. Methods Phys. Res., Sect. A* **422**, 484 (1999).
- [16] <http://www.rcnp.osaka-u.ac.jp>.
- [17] T. Noro *et al.*, in Research Center Nuclear Physics (Osaka University) Annual Report, 1991, p. 177.
- [18] Y. Fujita, K. Hatanaka, G.P.A. Berg, K. Hosono, N. Matsuoka, S. Morinobu, T. Noro, M. Sato, K. Tamura, and H. Ueno, *Nucl. Instrum. Methods Phys. Res., Sect. B* **126**, 274 (1997), and references therein.
- [19] H. Fujita *et al.*, *Nucl. Instrum. Methods Phys. Res., Sect. A* **484**, 17 (2002).
- [20] C. D. Goodman *et al.*, *Phys. Lett.* **107B**, 406 (1981).
- [21] J. Rapaport *et al.*, *Nucl. Phys.* **A410**, 371 (1983).
- [22] H. Fujita *et al.*, *Nucl. Instrum. Methods Phys. Res., Sect. A* **469**, 55 (2001).
- [23] T. Adachi *et al.*, *Phys. Rev. C* **85**, 024308 (2012).
- [24] T. Adachi *et al.*, *Phys. Rev. C* **73**, 024311 (2006).
- [25] Y. Fujita *et al.*, *Phys. Rev. Lett.* **95**, 212501 (2005).
- [26] F. Molina, B. Rubio, Y. Fujita, and W. Gelletly, *AIP Conf. Proc.* **1423**, 23 (2012).
- [27] Y. Fujita *et al.*, *Phys. Rev. C* **88**, 014308 (2013).
- [28] M. Honma, T. Otsuka, T. Mizusaki, M. Hjorth-Jensen, and B. A. Brown, *J. Phys. Conf. Ser.* **20**, 7 (2005), and references therein.
- [29] H. Toki and G. F. Bertsch, *Phys. Rev. C* **26**, 2330 (1982).
- [30] P. Sarriguren, *Phys. Rev. C* **87**, 045801 (2013).
- [31] G. F. Bertsch and Y. Luo, *Phys. Rev. C* **81**, 064320 (2010), and references therein.
- [32] J. Engel, M. Bender, J. Dobaczewski, W. Nazarewicz, and R. Surman, *Phys. Rev. C* **60**, 014302 (1999).
- [33] E. Moya de Guerra, A. A. Raduta, L. Zamick, and P. Sarriguren, *Nucl. Phys.* **A727**, 3 (2003).
- [34] A. O. Macchiavelli, in *Fifty Years of Nuclear BCS*, edited by R. A. Broglia and V. Zelevinsky (World Scientific, Singapore, 2013), Chap. 32, p. 432.
- [35] C. L. Bai, H. Sagawa, M. Sasano, T. Uesaka, K. Hagino, H. Q. Zhang, X. Z. Zhang, and F. R. Xu, *Phys. Lett. B* **719**, 116 (2013); C. L. Bai *et al.* (private communication).
- [36] T. Kurtukian Nieto *et al.*, *Phys. Rev. C* **80**, 035502 (2009).
- [37] E. P. Wigner, *Phys. Rev.* **51**, 106 (1937).
- [38] D. R. Tilley, C. M. Cheves, J. L. Godwin, G. M. Hale, H. M. Hofmann, J. H. Kelley, C. G. Sheu, and H. R. Weller, *Nucl. Phys.* **A708**, 3 (2002).
- [39] D. R. Tilley, H. R. Weller, C. M. Cheves, and R. M. Chasteler, *Nucl. Phys.* **A595**, 1 (1995).
- [40] B. D. Anderson *et al.*, *Phys. Rev. C* **27**, 1387 (1983).